Progress In Electromagnetics Research, PIER 17, 323–337, 1997

LEAKY FIELDS ON MICROSTRIP

L. O. McMillan, N. V. Shuley and P. W. Davis

Department of Electrical and Computer Engineering
The University of Queensland
Brisbane, Australia, 4072.

1. INTRODUCTION

The dispersion characteristic for microstrip has been investigated by a number of authors using different methods and evaluating different regimes of the dispersion characteristic. Ermert [1] first evaluated the propagation modes in the bound regime only, Oliner and Lee [2], Michalski and Zheng [3], Bagby et al. [4] extended the characteristic into the surface and radiation regimes.

In all of the earlier papers the authors have evaluated the dispersion characteristic and the current distributions excited on the microstrip LWA, but up until now no author has evaluated the electric fields which can exist in conjunction with a leaky mode excited on microstrip. Evaluation of the electric field allows the validation of the solution, as the boundary conditions used to formulate the problem can be checked.

In this paper a similar formulation to that presented by Bagby et al. [4] is used. Section 2 presents the varied formulation of an open microstrip transmission line. Section 3 gives a brief description of the

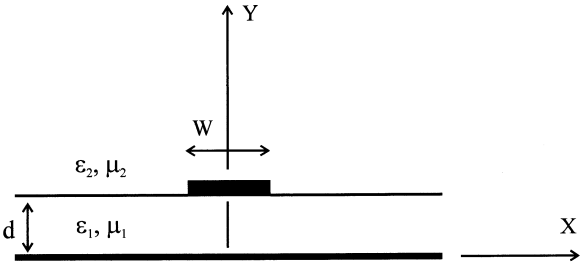

Figure 1. Geometry of open microstrip transmission line.

main differences between the three regimes of the dispersion characteristic. It is unclear from the literature what is the best choice of integration path and branch cuts, to solve the eigenvalue problem. Section 4 discusses the various considerations and options found in the literature. Section 5 presents a closed form result for the E field on the microstrip LWA. Results are presented and discussed in section 6.

2. FORMULATION

Consider the uniform open microstrip transmission line shown in Figure 1. This structure can be analysed by solving the coupled homogeneous integral equations [5]

$$\int_{-w/2}^{w/2} [Z_{zz}(x-x',y)J_z(x') + Z_{zx}(x-x',y)J_x(x')]dx' = E_z(x) \quad (1a)$$

$$\int_{-w/2}^{w/2} [Z_{xz}(x-x',y)J_z(x') + Z_{xx}(x-x',y)J_x(x')]dx' = E_x(x) \quad (1b)$$

Taking the Fourier transform w.r.t x of (1) and arranging in matrix form

$$\begin{bmatrix} \tilde{E}_z \\ \tilde{E}_x \end{bmatrix} = \begin{bmatrix} \tilde{Z}_{zz} & \tilde{Z}_{zx} \\ \tilde{Z}_{xz} & \tilde{Z}_{xx} \end{bmatrix} \begin{bmatrix} \tilde{J}_z \\ \tilde{J}_x \end{bmatrix} \quad (2)$$

where the Fourier transforms of the Green's functions $\tilde{Z}_{zz}, \tilde{Z}_{zx}, \tilde{Z}_{xz}$ and $\tilde{Z}_{xx}$ are given by

$$\tilde{Z}_{zz} = \frac{-1}{\alpha^2+\beta^2}\left[\beta^2\tilde{Z}_e + \alpha^2\tilde{Z}_h\right] \quad (3)$$

$$\tilde{Z}_{zx} = \tilde{Z}_{xz} = \frac{-\alpha\beta}{\alpha^2+\beta^2}\left[\tilde{Z}_e - \tilde{Z}_h\right] \tag{4}$$

$$\tilde{Z}_{xx} = \frac{-1}{\alpha^2+\beta^2}\left[\alpha^2\tilde{Z}_e + \beta^2\tilde{Z}_h\right] \tag{5}$$

where,

$$\tilde{Z}_e = \frac{1}{\frac{j\omega\epsilon_1}{\gamma_1}\coth(\gamma_1 d) + \frac{j\omega\epsilon_2}{\gamma_2}} \tag{6}$$

$$\tilde{Z}_h = \frac{1}{\frac{\gamma_1}{j\omega\mu_1}\coth(\gamma_1 d) + \frac{\gamma_2}{j\omega\mu_2}} \tag{7}$$

$$\gamma_i = \sqrt{\alpha^2+\beta^2-k_i^2} \qquad i = 1,2 \tag{8}$$

where β $(= \beta_r - j\beta_i)$ is the z directed propagation constant, α is the spectral variable and k_i is the free space propagation constant in medium i (refer Figure 1). Quantities with tildes are the Fourier transforms of the corresponding quantities.

The currents J_x and J_z are expanded in a series of Chebyshev polynomials of the first and second kind ($T_n(x)$, $U_n(x)$). Chebyshev polynomials are chosen as they are entire domain basis functions, which are easily modified to satisfy the edge conditions on microstrip. The Fourier transforms of these current functions are a weighted series of Bessel functions of the first kind.

$$J_z(x) = \frac{1}{\sqrt{1-(\frac{x}{w/2})^2}}\sum_{n=0}^{N} c_n T_n\left(\frac{x}{w/2}\right) \tag{9}$$

$$\tilde{J}_z(\alpha) = \sum_{n=0}^{N} c_n j^n \pi\frac{w}{2} J_n\left(\frac{w}{2}\alpha\right) \tag{10}$$

$$J_x(x) = \sqrt{1-(\frac{x}{w/2})^2}\sum_{m=0}^{M} d_m U_m\left(\frac{x}{w/2}\right) \tag{11}$$

$$\tilde{J}_x(\alpha) = \sum_{m=0}^{M} d_m \frac{j^m\pi(m+1)}{\alpha} J_{m+1}\left(\frac{w}{2}\alpha\right) \tag{12}$$

The J_{m+1}, J_n in (10) and (12) are Bessel functions not currents.

Applying Galerkin's method and Parseval's theorem to (2) will result in a matrix equation with unknown coefficients c_n and d_m and β.

$$[K][c_n \quad d_m]^T = \vec{0} \tag{13}$$

$$K^{(a,b)} = \int_0^\infty \tilde{J}_a(\alpha)\tilde{Z}_{ab}(\alpha,\beta)\tilde{J}_b(\alpha)d\alpha \tag{14}$$

$$a = x, z$$

$$b = x, z$$

The limits of integration in (14) are from 0 to ∞ instead of $-\infty$ to ∞. This is due to a symmetry property of (14).

To ensure non trivial solutions of c_n and d_m, the determinant of $[K]$ must equal zero. The propagation constant β is evaluated, by finding a β which satisfies this condition.

3. DISPERSION CHARACTERISTIC

There are three propagation regimes on microstrip. The bound regime is where the E field is bound to the structure, and no energy is lost from the structure in the form of surface or space waves. In the surface wave region energy is lost from the structure in the form of a surface wave, which is bound to the surface of the dielectric, and propagates at an angle to the z axis (refer Figure 1). The radiation regime is the regime where leaky waves exist, and energy is radiated from the structure in the form of a space wave.

Strictly speaking, the surface wave and radiation regimes can be considered as the leaky regime, since energy is leaked from the transmission line. In this paper, the leaky region is associated with the radiation regime.

These regimes are separated by the nature of the propagation constant and by the pole and branch point locations in the complex α plane. The bound regime is characterised by $Re\{\beta^2\} > Re\{TM_o^2\} > Re\{k_2^2\}$. The surface wave regime is characterised by $Re\{TM_o^2\} > Re\{\beta^2\} > Re\{k_2^2\}$. The radiation regime is characterised by $Re\{k_2^2\} > Re\{\beta^2\}$ [4].

4. PATHS OF INTEGRATION

The matrix elements which make up the entries of the K matrix (14), for the situation of bound modes, are all integrals along the real axis in the α plane, and are easy to evaluate. Figure 2 shows the pole and branch cut locations for this case, and it can be noted that there are no obstructions to the path of integration.

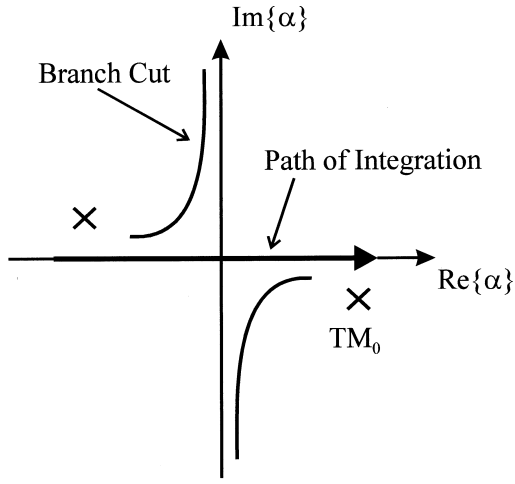

Figure 2. Pole and branch cut locations in the α plane for the bound regime. Integration path is along the real α axis.

For the situation of leaky modes, the Surface wave poles (due to the TM_o mode) and branch points due to the square root function associated with (8) cross the real axis. These discontinuities do not interfere with the real axis (refer Figure 3), and therefore one could assume that the path of integration would be the same as the path used for the evaluation of bound modes, however this would be an incorrect assumption. In order to maintain physical continuity of the fields in passing from the non leaky to the leaky regions, the integration path must stay on the same side of both the branch point and the pole (ie. above them). This then leads to the path of integration shown in Figure 3. The fact that the path of integration passes through the branch cut indicates that the integral will violate Cauchy's Integration theorem, but it will obey Sommerfeld's radiation condition. The part of the path of integration in Figure 3, which lies between the two branch cuts

is where γ (8) is evaluated on the bottom Riemann sheet. Allowing the path of integration to pass across the branch cut onto the bottom sheet gives a contribution to the integral which comes from the Leaky mode which we are looking for.

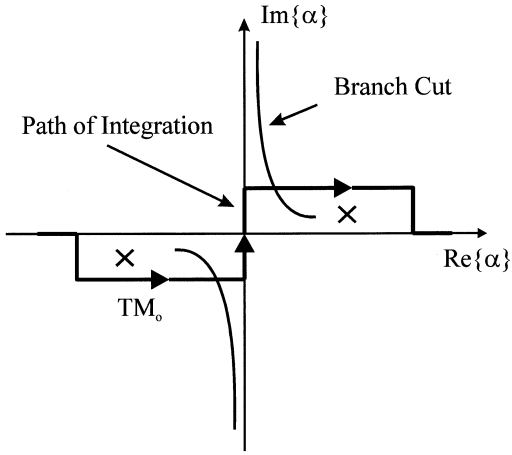

Figure 3. Pole and branch cut locations in the α plane of the leaky regime. Path of integration is indicated.

It can be noted that the branch cuts in Figure 2 and 3 approach the imaginary axis from different sides (they have been inverted). This situation troubled some authors [6] as the integration path in Figure 3 crossed the branch cut and violated Cauchy's Integration Theorem. Their solution to this dilemma was to make the branch cut asymptotic to the same side of the imaginary axis as the parameters changed to move the branch point across the real axis, refer Figure 4. This then ensures that the path of integration does not pass through the branch cuts. The branch cuts shown in Figure 4 do not represent a set of Riemann sheets which separate the top and bottom sheets by setting the imaginary part of γ^2 to equal zero. These new branch cuts allow growing waves over a portion of the α plane between the branch cuts (refer Figure 4). This portion lies in the middle of the integration path in Figure 4 and gives a similar contribution to the integral as was achieved previously by integrating along the bottom Riemann sheet.

The results given in this paper are found using the option of integrating through the branch cut. This was due to the simplicity of implementing this method numerically.

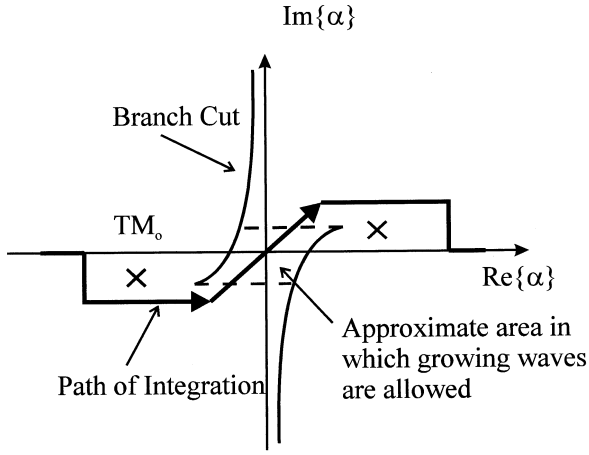

Figure 4. Alternative branch cuts.

The path of integration was chosen such that it minimised the chance of being too close to any leaky wave (LW) poles. If a LW pole is encountered, then the path would need to be deformed appropriately to capture the pole. In the course of solving for the leaky modes, no LW poles interfered with the path of integration.

5. FIELDS

Closed form equations for the transformed cross sectional fields excited on open microstrip are derived from the spectral domain analysis (15)–(20). The exponential time variation $e^{j\omega t}$ is suppressed. The subscripts 1 and 2 refer to the dielectric and air regions respectively (refer Figure 1).

$$\tilde{E}_{x1}(\alpha, y) = \frac{\sinh(\gamma_1 y)}{\sinh(\gamma_1 d)} \left[\tilde{Z}_{xz}\tilde{J}_z + \tilde{Z}_{xx}\tilde{J}_x\right] e^{-j\beta z} \tag{15}$$

$$\tilde{E}_{y1}(\alpha, y) = -\frac{\cosh(\gamma_1 y)}{\sinh(\gamma_1 d)} \frac{1}{\gamma_1} \left[j\beta\tilde{Z}_e\tilde{J}_z + j\alpha\tilde{Z}_e\tilde{J}_x\right] e^{-j\beta z} \tag{16}$$

$$\tilde{E}_{z1}(\alpha, y) = \frac{\sinh(\gamma_1 y)}{\sinh(\gamma_1 d)} \left[\tilde{Z}_{zz}\tilde{J}_z + \tilde{Z}_{zx}\tilde{J}_x\right] e^{-j\beta z} \tag{17}$$

$$\tilde{E}_{x2}(\alpha, y) = e^{(-\gamma_2(y-d))} \left[\tilde{Z}_{xz}\tilde{J}_z + \tilde{Z}_{xx}\tilde{J}_x\right] e^{-j\beta z} \tag{18}$$

$$\tilde{E}_{y2}(\alpha, y) = e^{(-\gamma_2(y-d))} \frac{1}{\gamma_2} \left[j\beta \tilde{Z}_e \tilde{J}_z + j\alpha \tilde{Z}_e \tilde{J}_x \right] e^{-j\beta z} \tag{19}$$

$$\tilde{E}_{z2}(\alpha, y) = e^{(-\gamma_2(y-d))} \left[\tilde{Z}_{zz} \tilde{J}_z + \tilde{Z}_{zx} \tilde{J}_x \right] e^{-j\beta z} \tag{20}$$

Evaluation of the electric field in the spatial domain involves inverse transforming the above quantities. To evaluate the fields correctly, the same integration path used to solve the propagation constant must be followed for the evaluation of the fields. This simply follows on from the concept of maintaining the physical continuity of the problem. In the case of a bound mode, a discrete fast Fourier transform (FFT) approach can be used, which is computationally very efficient.

Application of the FFT for the evaluation of electric fields which are excited by a leaky mode is quite complex. Applying the FFT to the integration path shown in Figure 3 requires the use of a Schwartz-Christoffel transform, to map the integration path of Figure 3 to the real axis of another plane (Q Plane). The FFT can then be applied in the Q plane. The mapping between the α plane and the Q plane is defined by equation (21). Equation (21) has a simple relationship between the Q plane and the α plane, but the reverse relationship is not easy to compute. This fact makes the application of the FFT for evaluating leaky electric fields quite difficult.

$$\alpha = \frac{j4X_c}{\pi} \left(\sin^{-1} \sqrt{Q} + \sqrt{Q(1-Q)} \right) - jX_c \tag{21}$$

where X_c is a constant associated with the path of integration.

The E fields for leaky modes are determined by evaluating the Fourier transform via numerical integration. The path of integration used is given in Figure 3. This particular approach is computationally more intensive than the discrete Fourier transform approach.

6. RESULTS

The results presented in this paper (Figures 5–14) are evaluated using microstrip parameters: relative permittivity of substrate = 2.32, thickness of the dielectric = 0.794 mm and the width of the strip = 15 mm.

Observation of the electric field plots (Figures 5–14) shows that there is no dramatic difference between the bound and leaky E_x and E_z fields excited on microstrip, except for the magnitude and rate of decay of the field away from the strip. The E_z field seems to be less

tightly confined to the strip for the leaky field, compared to the bound field. This is not a surprising result, since this allows the transfer of energy from the excited leaky wave field on the antenna to the radiated field.

In order for the cross sectional electric fields presented in this paper to be valid solutions, the fields must obey the boundary condition on the air dielectric interface. The boundary condition on the ground plane is taken care of in the field equations (15)–(17). The E_x and E_z fields show that the field over the metalization is in most Ex plots is zero, and it is small compared to the field outside the strip for the E_z plots. The small field on the strip can be accounted for by not using enough basis functions to promote full convergence of the electric field. The number of basis functions used to generate all of the data in this paper were $N = 4$ and $M = 3$. This number of basis functions provided good convergence for the propagation constant, and current solutions, however more basis functions should be used to fully converge the E_z field. Increasing the number of basis functions increases the computation time significantly.

7. CONCLUSION

A spectral domain integral equation formulation is presented for the evaluation of propagation constants, currents and fields excited on a microstrip transmission line, when the transmission line is operating in any of the three propagation regions.

Considerations when choosing the paths of integration for the various propagation regimes are discussed. The method of integrating through the branch cut (for leaky modes) is used in this paper, as it was found to be the simplest to implement numerically.

The electric field solutions obtained from the formulas (15)–(20) are correct because all the boundary conditions are satisfied and hence, within the limits of convergence, the formulas (15)–(20) provide a correct solution.

The electric field distributions are found not to alter significantly as the operating regime is changed from bound to leaky (or leaky to bound).

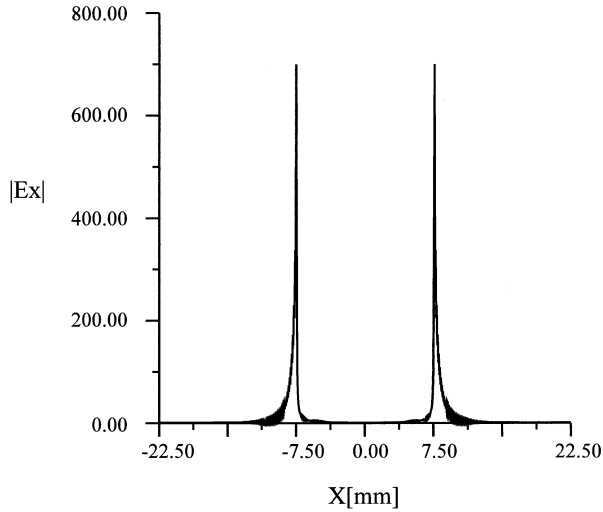

Figure 5. X component of the Electric field on the air-dielectric interface for the Dominant mode. (frequency = 5 GHz).

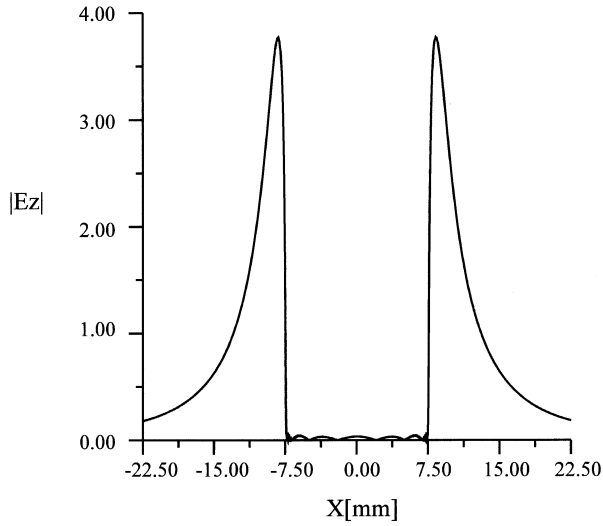

Figure 6. Z component of the Electric field on the air-dielectric interface for the Dominant mode. (frequency = 5 GHz).

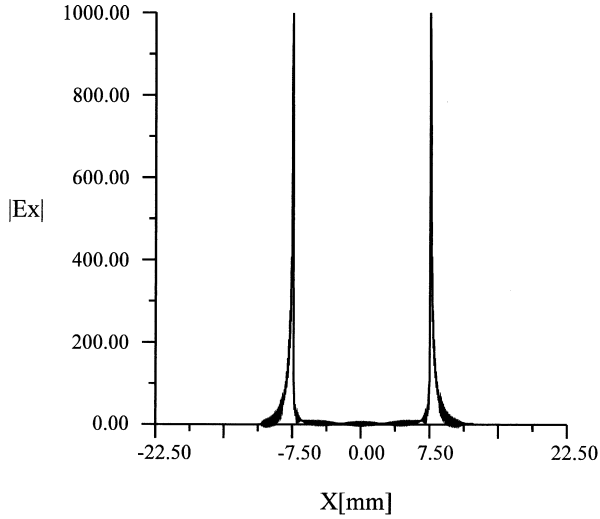

Figure 7. X component of the Electric field on the air-dielectric interface for the EH_1 bound mode. (frequency = 14 GHz).

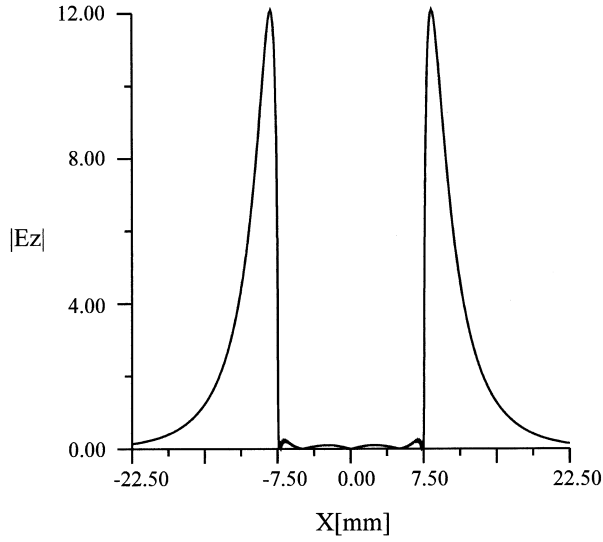

Figure 8. Z component of the Electric field on the air-dielectric interface for the EH_1 bound mode. (frequency = 14 GHz).

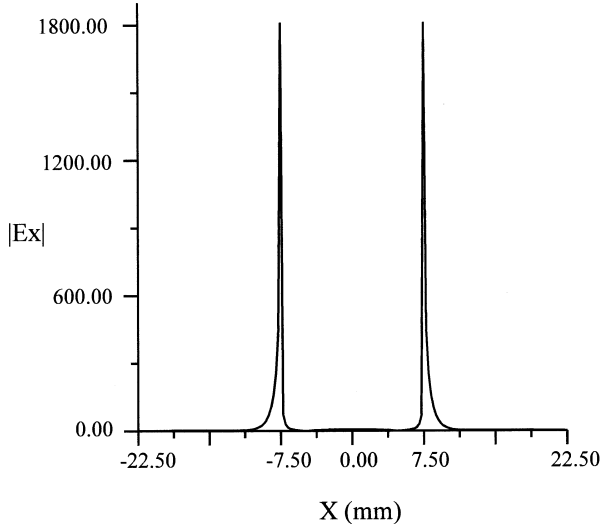

Figure 9. X component of the Electric field on the air-dielectric interface for the EH_1 leaky mode. (frequency = 7 GHz).

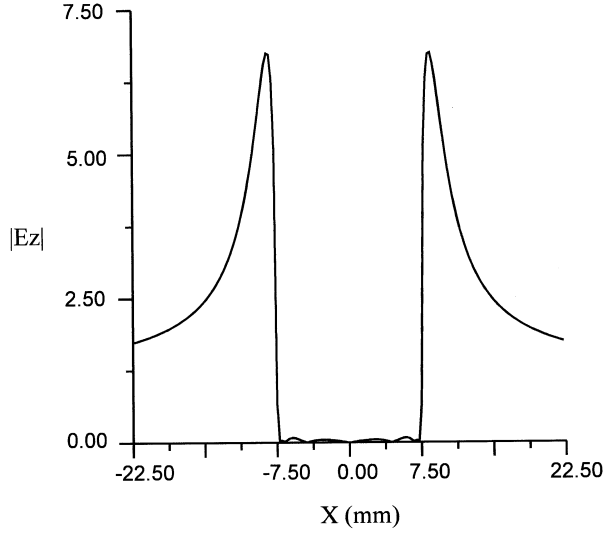

Figure 10. Z component of the Electric field on the air-dielectric interface for the EH_1 leaky mode. (frequency = 7 GHz).

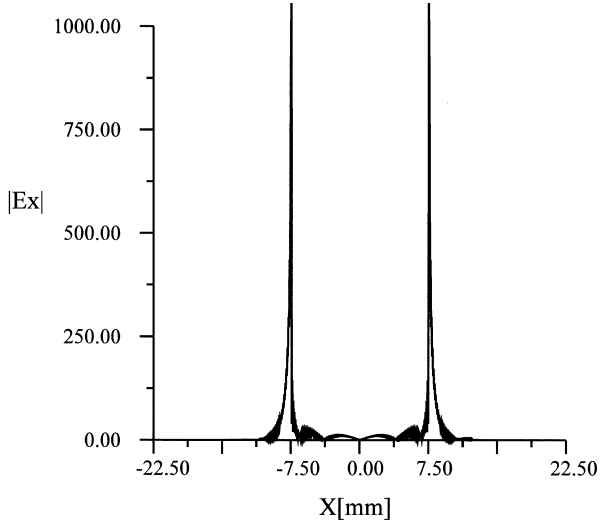

Figure 11. X component of the Electric field on the air-dielectric interface for the EH_2 bound mode. (frequency = 24 GHz).

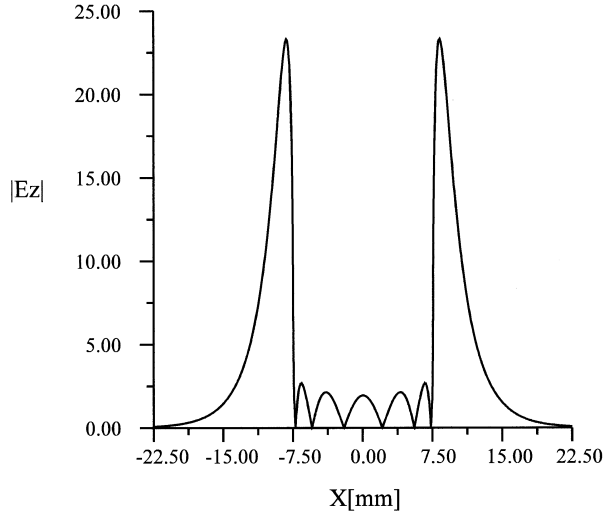

Figure 12. Z component of the Electric field on the air-dielectric interface for the EH_2 bound mode. (frequency = 24 GHz)

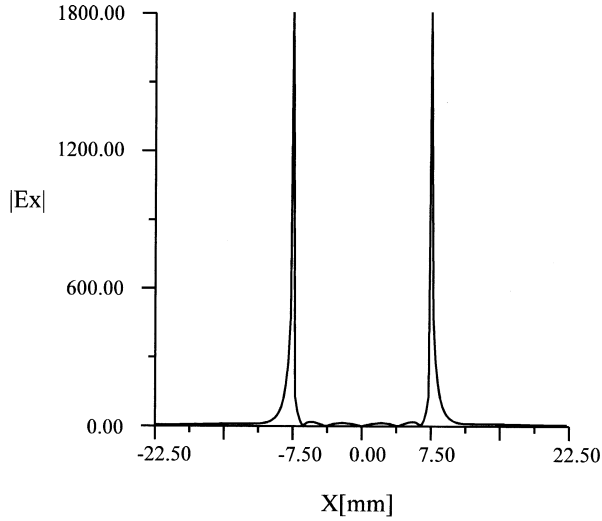

Figure 13. X component of the Electric field on the air-dielectric interface for the EH_2 leaky mode. (frequency = 14 GHz)

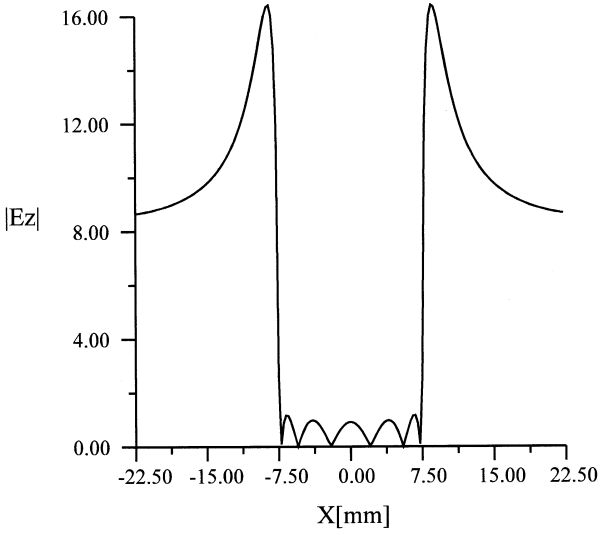

Figure 14. Z component of the Electric field on the air-dielectric interface for the EH_2 leaky mode. (frequency = 14 GHz)

REFERENCES

1. Ermert, H. "Guided modes and radiation characteristics of covered microstrip lines," A.E.U. Band 30, 65–70, 1976.
2. Oliner, A. A. and K. S. Lee, "Scannable millimeter wave arrays," Technical report, Polytechinc University, 1988 .
3. Michalski, K. A. and D. Zheng, "On the leaky modes of open microstrip lines," *Microwave and Optical Technology Letters,* Vol. 2, 6–8, 1989.
4. Bagby, J. S., C. H. Lee, D. P. Nyquist, and Y. Yuan, "Identification of propagation regimes on integrated microstrip transmission lines," *IEEE Trans. MTT,* Vol. 41, 1887–1893, 1993.
5. Itoh, T. Numerical Techniques for Microwave and Millimetre Wave Passive Structures, Wiley, 1989.
6. Grim J. M. and D. P. Nyquist, "Spectral analysis considerations relevant to radiation and leaky modes of open-boundary microstrip transmission line," *IEEE Trans. MTT,* Vol. 41, 150–153, 1993.